Chapter 2. Experimental

2.1. Synthesis

A number of methods were studied in this thesis. The preparation of clear gel solution was the first step of all these methods. The obtained solutions were then processed in different procedures depending on the method applied. The use of the same starting solution among these methods can provide the ease of comparison between them (Figure 2.1).

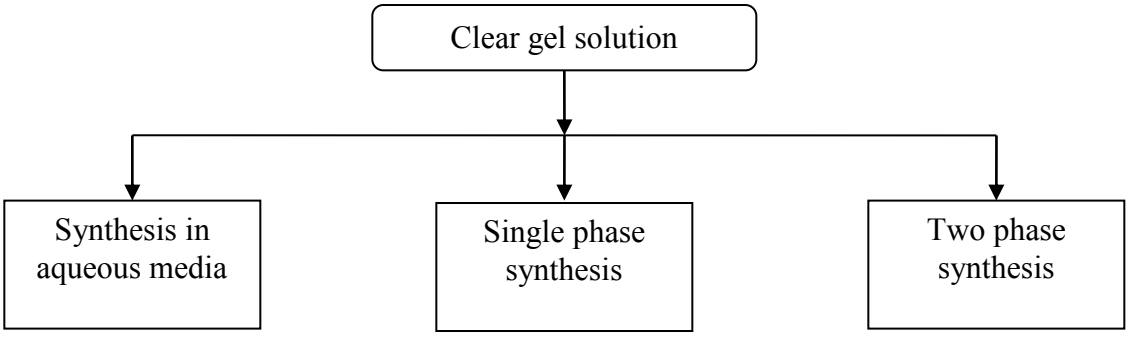

Figure 2.1. Methods studied for the synthesis of nanozeolites

2.1.1. Preparation of clear zeolite gel solution

Silicalite-1

In a typical recipe according to Trong-On Do et al,[1] 14 g of tetrapropylammonium hydroxide (TPAOH) 20% in water was added to 7.8 g of tetraorthosilicate $Si(OC_2H_5)_4$. The mixture was stirred vigorously for 24 h at room temperature. The molar gel composition was: 2.68 SiO_2 : 1 TPAOH : 168 H_2O.

FAU zeolites

The preparation of clear synthesis solution for FAU nanozeolites followed Mintova et al.[2] First a 38.4 g solution of NaOH 0.05 N (Fischer) was diluted with 121.6 g H_2O. Then 52.3 g tetramethylammonium hydroxide solution (Aldrich, 25% in water) and aluminium isopropoxide, $Al(iPr)_3$, (Aldrich, 98%) were added in that order, and stirred vigorously until the solution became clear. To this solution 21.66 g of tetraorthosilicate was added. This clear solution was aged for 3 days under vigorous stirring at room temperature. The final molar composition was: 2.46 $(TMA)_2O$: 0.032 Na_2O : 1 Al_2O_3 : 3.4 SiO_2 : 370 H_2O.

2.1.2. Synthesis of nanozeolites using clear gel solution in aqueous medium (conventional method)

In this method, a Teflon-lined stainless steel autoclave (Figure 2.2) was employed to perform the crystallization under hydrothermal conditions. Before use, the Teflon beaker was cleaned by immersing in hydrofluoric acid (HF, 20%) for 24 h, and then washed with distilled water. This is to remove the crystalline residue on the surface of the Teflon beaker from previous synthesis. After being filled with the prepared clear solution, the autoclave was completely sealed and heated in a convection oven at desired temperature.

For the synthesis of silicalite-1, the temperature was 100^oC and the crystallization time was 24 h, whereas, for that of FAU zeolites, the temperature and crystallization time were 100^oC and 6 days, respectively.

The solid product was recovered by centrifugation at the speed of 20.000 rpm for 1 h, washed several times with distilled water, dried over night at 80 ^oC, and calcined in air at 550 ^oC for 8 h.

In this thesis the zeolites produced using this method were referred to as reference samples or nanozeolites synthesized using conventional method.

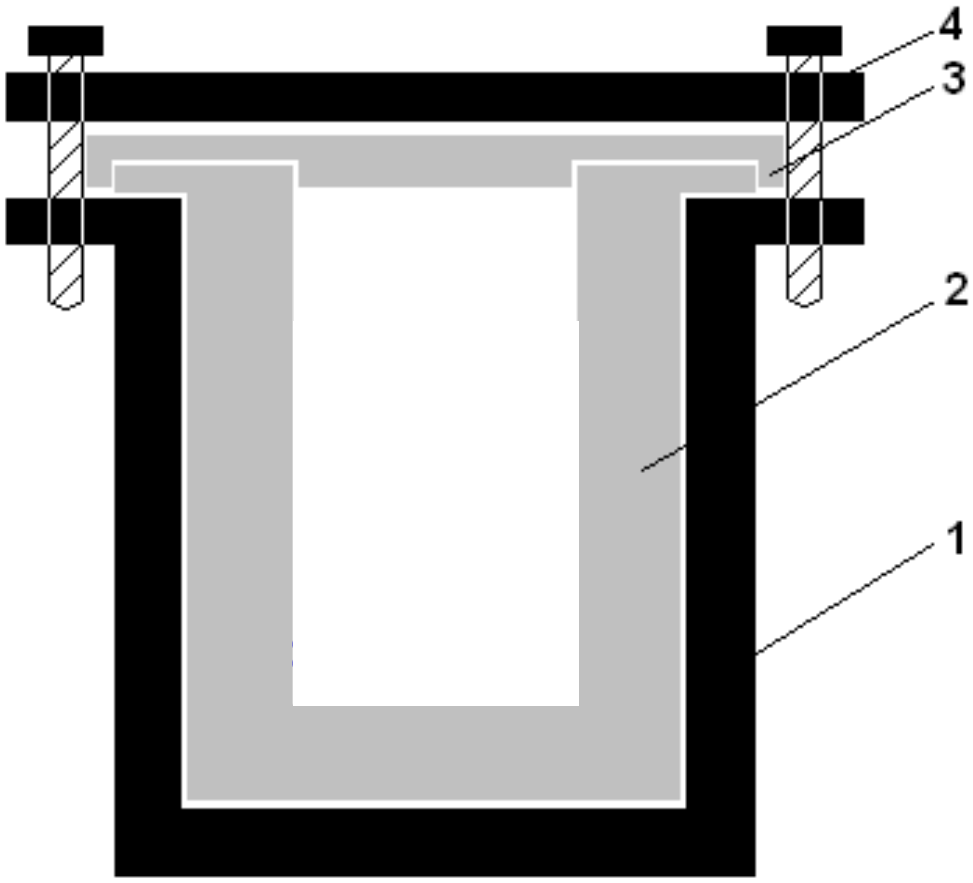

Figure 2.2. Scheme of the autoclave: (1) a cylindrical stainless steel vessel, (2) a Teflon cylindrical beaker, (3) a flat Teflon cover for closing the Teflon beaker, (4) a flat stainless steel cover which was tightened up to part (1) by six screws.[3]

2.1.3. Synthesis of nanozeolites in organic medium

2.1.3.1. Synthesis of nanozeolites using single-phase method

The procedure is consisted of the following steps:

(i) Preparing a clear zeolite gel solution. This clear gel was heated at 80ºC for 12 hours to produce zeolite seeds.

(ii) To this clear zeolite gel solution, an organic solvent containing organosilanes was added and stirred for several hours at 40-100ºC.

(iii) The organic phase containing organosilane-functionalized zeolite seeds was extracted. This organic phase was transferred into an autoclave and then heated at desired temperature for crystallization.

(iv) After the crystallization, the resulting nanozeolite product was recovered by centrifugation and then washed with ethanol and water for several times. The product was then dried at 80ºC for 24 hours and calcined at 550ºC for 5 hours.

Typically, 10 g of zeolite gel solution was added to 500 ml of a solution of toluene containing n-butanol (30% wt) and a certain amount of hexadecyltrimethoxysilane. The organosilane was in a proportion of less than 10% mol in regards to the silica content in the gel. After vigorous stirring at 60 ^{o}C for 48 h a mixture clear to naked eyes was obtained. This mixture was then transferred to an autoclave for further hydrothermal treatment at 150^{o}C for 3 days and 170^{o}C for 1 day for faujasite and silicalite-1, respectively.

2.1.3.2. Synthesis of nanozeolites using two-phase method

The procedure is consisted of the following steps

i) Preparing a clear zeolite gel solution. This clear solution was heated at 80 ºC for 12 hours to produce zeolite seeds.

ii) To this clear solution, an organic solvent (such as n-octane, toluene, etc.) containing oganosilanes (for example, hexadecyltrimethoxysilane) in an organic solvent was added. The organosilane was in proportion of less than 10% mol with respect to the silica content in the gel. Since the solvent is insoluble in water, a two-phase system was obtained and was stirred for 12 hours at 80 ºC.

iii) The two-phase mixture was transferred into an autoclave and then heated at elevated temperature (100-200 ºC) for crystallization.

iv) After the crystallization, the organic phase containing organosilane-functionalized nanozeolite was extracted. In the organic phase, the resulting nanozeolite product was recovered by centrifugation and then washed with ethanol and water for several times. The product was then dried at 80 ºC for 24 hours and calcined at 550 ºC for 5 hours.

For the synthesis of nanosilicalite-1, typically, 21.8 g of clear zeolite gel solution was heated at 80^{o}C for 12 h, the obtained solution was added with 93 g of a solution of toluene containing 1.22% wt hexadecyltrimethoxysilane, resulting in a two-phase mixture. After stirring for 12 hours at 60^{o}C, the organic phase mixture was extracted and transferred into an autoclave; and heated at 170^{o}C for 24 hours.

2.1.4. Preparation of silica containing nanozeolites

Two types of silica containing zeolites which had the zeolite content of 20 %wt and 50% wt respectively were prepared. These two samples were referred to as nano-faujasite-20 and nano-faujasite-50, respectively. Typically, for the synthesis of silica containing 20%wt zeolite, 30 g of distilled water was added with 100 g of ethanol (Aldrich 98%) under stirring. Next, 14.16 g of TEOS (Aldrich, 98%) was added and stirred until the solution became clear. Subsequently, 1 g of FAU nanozeolite, which was prepared using conventional method, was added. The obtained mixture was then heated at 80 ^{o}C with reflux under vigorous stirring overnight. The product was separated by filtration and washed with distilled water for several times, dried overnight at 120 ^{o}C, then calcined at 550 ^{o}C for 8 h.

2.1.5. Synthesis of MIL-88B metal-organic framework

In a typical synthesis, 0.67 mmol of $FeCl_3.6H_2O$ 99%, 0.33 mmol of corresponding $Ni(NO_3)_2.6H_2O$ 97% and 1 mmol of bdc 98% were dissolved in 10 ml of DMF. To this clear solution, 0.4 mmol of NaOH was added under stirring for 15 min. The mixture was then transferred into a Teflon-lined autoclave and heated at 100 ^{o}C for 15 h. Solid product was then recovered by filtration and washed several times with DMF. The sample was treated with water, pyridine (Py), pyrazine (Pz) and 4-,4'-bipyridine (Bp) to obtain Fe_2Ni-MIL-88B.H_2O, Fe_2Ni-MIL-88B.Py, Fe_2Ni-MIL-88B.Pz and Fe_2Ni-MIL-88B.Bp, respectively (see Supporting Information). For comparison, the single metal Fe_3-MIL-88B.DMF was also prepared using the procedure of Férey et al

For the mechanism investigation of MIL-88B the syntheses have the same molar ratios with respect to the metal cluster (Fe_3O or Fe_2NiO). In addition, the molar ratio of bdc (benezendicarboxylic) over metal cluster is kept stoichiometric (and is of 3). Single metal

synthesis: vials of 10 ml DMF solution of 10 mmol of $FeCl_3.6H_2O$ 99% or $Fe(NO_3)_3.9H_2O$ 98% were added with 10 mmol bdc under stirring. Next 4 ml of NaOH 2M was rapidly injected with continuous stirring. The vials were then capped and heated at 100 ^oC for different times: 0 h (5 min after the addition of NaOH at room temperature), 1h, 2h, 3h, and 12 h. Mixed metal synthesis: vials of 10 ml DMF solution of 3,33 mmol of $Ni(NO_3)_2.6H_2O$ and 6.67 mmol of $FeCl_3.6H_2O$ 99% or $Fe(NO_3)_3.9H_2O$ 98% were added with 10 mmol bdc under stirring. Next 4 ml of NaOH 2M was rapidly injected with continuous stirring. The vials were then capped and heated at 100 ^oC for different times: 0 h (5 min after the addition of NaOH at room temperature), 1h, 2h, 3h, and 12 h. Solids products were recovered by centrifugation at 5000 rpm for 5 min. The solids were then dried in vacuum for 24 h at 50 ^oC. In general, the samples prepared with $FeCl_3.6H_2O$ yield firm solids. However, those prepared with $Fe(NO_3)_3.9H_2O$ become thick gel during the heat treatment and thus, their corresponding solid products are not as firm as the solids from the Cl^- based samples.

2.2. Characterization

2.2.1. FTIR Spectroscopy

Fourier transform infrared spectroscopy (FTIR) is the subset of spectroscopy that deals with the infrared part of the electromagnetic spectrum; it can be used to identify a compound and to investigate the composition of a sample. Typically, when a molecule is exposed to infra-red (IR) radiation, it absorbs specific frequencies of radiation. The frequencies which are absorbed are dependent upon the functional groups within the molecule and the symmetry of the molecule. IR radiation can only be absorbed by bonds within a molecule, if the radiation has exactly the right energy to induce a vibration of the bond. This is the reason why only specific frequencies are absorbed.

Infrared spectroscopy focuses on the frequency range 400 - 4000 cm^{-1}, where cm^{-1} is known as wavenumber (1/wavelength), which is a unit of measure for the frequency. To generate the infrared spectrum, radiation containing all frequencies in the IR region is passed through the sample. Those frequencies which are absorbed appear as a decrease in the detected signal. This information is displayed as a spectrum of percentage transmitted

radiation plotted against wavenumber. When determining structure types of zeolites, the region of 400-1400 cm^{-1} is interesting. This region contains the framework vibrations of zeolite structure, and stretching and bending modes of the silica-alumina TO_4 tetrahedra. The framework vibrations of zeolite-type materials can be divided into structure insensitive and structure sensitive vibrations, as shown in Table 2.1. For the MIL-88B, the region of 400 – 800 cm^{-1} is important since it includes the vibrations of the metal clusters (Table 2.2).

Table 2.1. Structure insensitive and sensitive framework vibrations of zeolites [4]

Structure insensitive vibrations	**Wavenumber (cm^{-1})**
Asymmetric stretching vibrations	1200 – 1000
Symmetric stretching vibrations	850 – 700
Bending vibrations	600 – 400
Structure sensitive vibrations	**Wavenumber (cm^{-1})**
Asymmetric stretching vibrations	1050 – 1150
Symmetric stretching vibrations	750 – 820
Double ring vibrations	500 – 650
Pore opening vibrations	300 – 420

Table 2.2. FTIR band assignment in the wavenumber 400 – 800 cm^{-1}

Band (cm^{-1})	**Assignment**
750	C-H[5, 6]
720	Fe_2NiO[7, 8]
690	C-C[5, 6]
660	OCO[5, 6]
624	Fe_3O[9, 10]
550	Fe-O, Ni-O[11]

To measure a sample, 1 mg of the sample was well-mixed with 99 mg of KBr powder (1 % sample in KBr) by grinding using an agate mortar and pestle. The obtained

powder was then crushed in a mechanical die press to form a translucent wafer. Finally, the wafer was placed in a FTIR spectrometer for measurement. A pure KBr wafer was also made for the background corrections.

2.2.2. Raman spectroscopy

The Raman scattering technique is a vibrational molecular spectroscopy which is derived from an inelastic light scattering process. With Raman spectroscopy, a laser photon is scattered by a sample molecule and loses (or gains) energy during the process. The amount of energy lost is seen as a change in energy (wavelength) of the irradiating photon. This energy loss is characteristic for a particular bond in the molecule. Raman can provide a precise spectral fingerprint, unique to a molecule or an individual molecular structure. In this respect it is similar to the more commonly found FT-IR spectroscopy. Raman analysis was carried out with a Horiba U100 Raman spectrometer using excitation wavelength of 514 nm.

2.2.3. UV-Vis spectroscopy

While IR and Raman spectroscopy techniques allow studying the vibrations of the atoms and the molecules, the UV-Vis (ultraviolet and visible, with the wavelength ranging from 200 to 800 nm) spectroscopy provides information about the electron transition inside them. When continuous radiation strike a material, a portion of the radiation may be absorbed. If that occurs, the residual or reluctant radiation, when it is passed through a prism, yields a spectrum with gaps in it, called an absorption spectrum. As a result of energy absorption, atoms or molecules pass from a state of low energy (the initial, or ground state) to a state of higher energy (the excited state). Figure 2.3 depicts this excitation process, which is quantized.

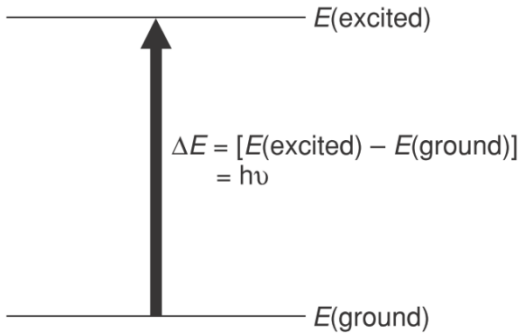

Figure 2.3. The excitation process

The electromagnetic radiation that is absorbed has energy exactly equal to the energy difference between the excited and ground states. In the case of ultraviolet and visible spectroscopy, the transitions that result in the absorption of electromagnetic radiation in this region of the spectrum are transitions between electronic energy levels. As a molecule absorbs energy, an electron is promoted from an occupied orbital to an unoccupied orbital of greater potential energy. Generally, the most probable transition is from the highest occupied molecular orbital (HOMO) to the lowest unoccupied molecular orbital (LUMO). The energy differences between electronic levels in most molecules vary from 125 to 650 kJ/mole (kilojoules per mole).

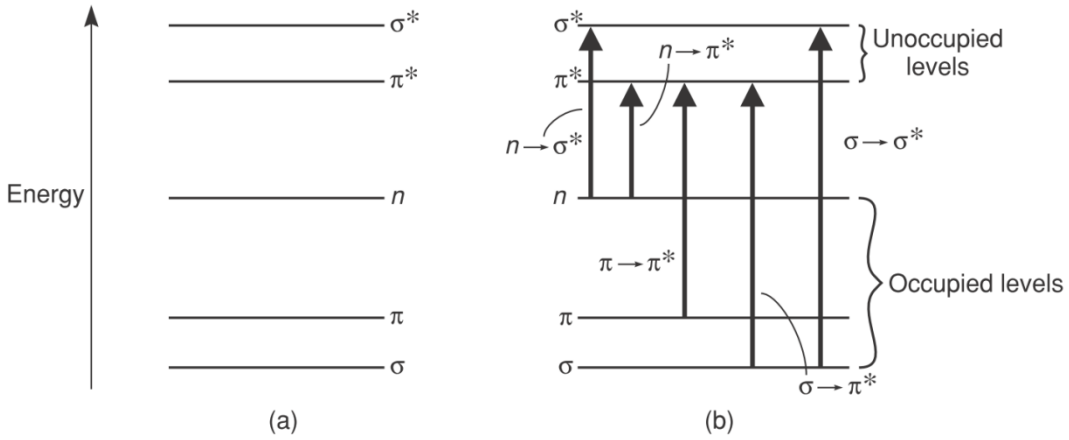

Figure 2.4. Electronic energy levels and transitions.

For most molecules, the lowest-energy occupied molecular orbitals are the σ orbitals, which correspond to s bonds. The π orbitals lie at somewhat higher energy levels, and orbitals that holdunshared pairs, the nonbonding (n) orbitals, lie at even higher energies. The unoccupied, or antibonding orbitals (π* andσ*), are the orbitals of highest energy. Figure 2.4a shows a typical progression of electronic energy levels. In all compounds other than alkanes, the electrons may undergo several possible transitions of different energies. Some of the most important transitions are

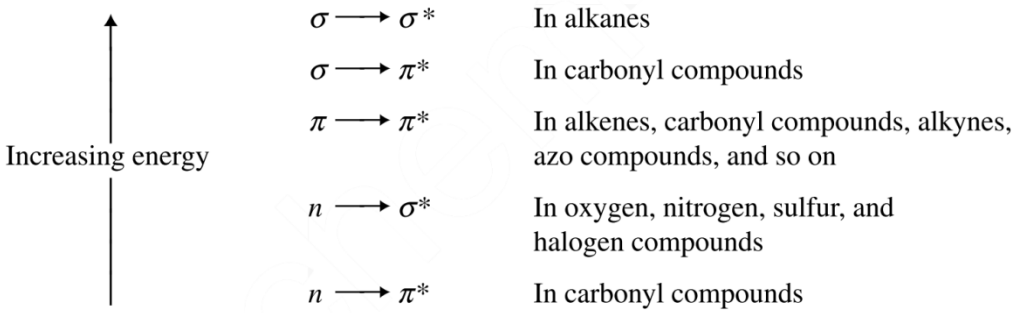

Figure 2.4b illustrates these transitions. Clearly, the energy required to bring about transitions from the highest occupied energy level (HOMO) in the ground state to the lowest unoccupied energy level (LUMO) is less than the energy required to bring about a transition from a lower occupied energy level. Thus, in Figure 2.4b an $n \rightarrow \pi^*$ transition would have a lower energy than a $\pi \rightarrow \pi^*$ transition. For many purposes, the transition of lowest energy is the most important. For transition metal complex the UV-Vis spectra can yield information about the d – d transfer and the charge transfer band. In our study, UV-Vis analysis was carried out in a Cary 300 instrument, using MgO wafer.

2.2.4. Energy-dispersive X-ray spectroscopy

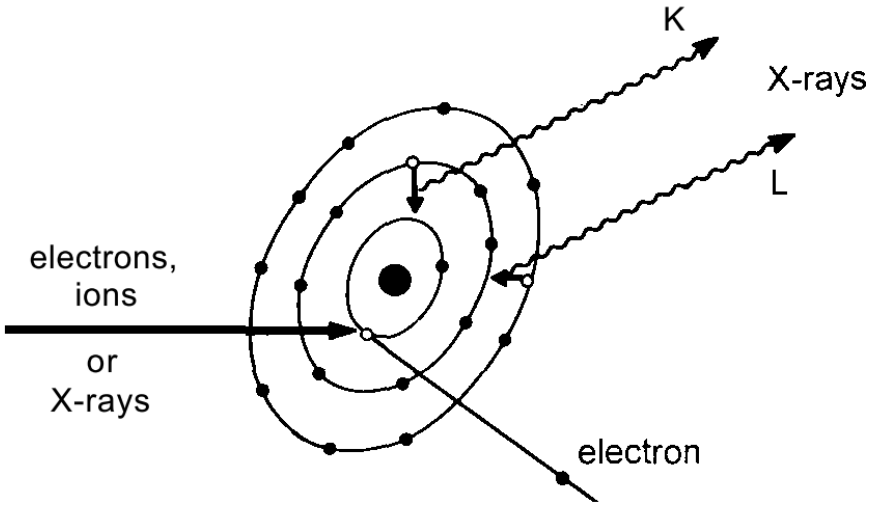

Figure 2.5. Principle of EDX spectroscopy

Energy-dispersive X-ray spectroscopy (EDX) is an analytical technique used for the elemental analysis or chemical characterization of a sample. When a high-energy beam of charged particles such as electrons or protons, or a beam of X-rays, is focused into the sample being studied, the incident beam may excite an electron in an inner shell of the atoms, ejecting it from the shell while creating an electron hole where the electron was. An electron from an outer, higher-energy shell then fills the hole, and the energy released from this may be released in the form of an X-ray. The number and energy of the X-rays emitted from a specimen can be measured by an energy-dispersive spectrometer. As the energy of the X-rays is characteristic of the difference in energy between the two shells, and of the atomic structure of the element from which they were emitted, this allows the elemental composition of the specimen to be measured. The EDX analysis was carried out using the Tecnai G2 F20 200 kV scanning transmission electron microscope. The probe diameter is about 3 nm and the acquiring time was set to 200 s.

2.2.5. X-ray Diffraction (XRD)

X-ray Diffraction (XRD) is a technique in crystallography in which the pattern produced by the diffraction of X-rays through the closely spaced lattice of atoms in a

crystal is recorded and then analyzed to reveal the nature of that lattice. XRD is a powerful technique for determining zeolite structure. Moreover, sample preparation is relatively easy, and the test itself is often rapid and non-destructive.

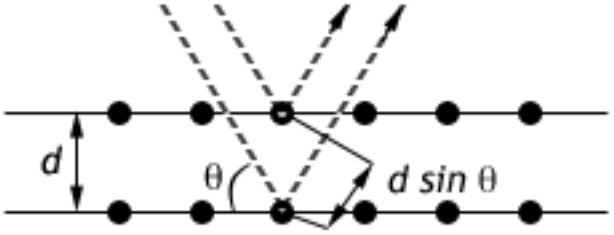

Figure 2.6. Diffraction of X-ray beams on a crystal lattice

The mechanism of XRD was well explained by Bragg in 1913.[12] A crystal can be considered to be composed of discrete parallel planes or layers of atoms. As the wave enters the crystal, it will be partially reflected by the first layer of atoms, while the rest of it will continue through to the second layer, where the process continues. The separately reflected waves will remain in phase if the difference in the path length of each wave ($2d\sin\theta$) is equal to an integer multiple of the wavelength ($n\lambda$) (Figure 2.6).

$$2d\sin\theta = n\lambda \tag{2.1}$$

This equation is known as Bragg's law, where:

- n is an integer,

- λ is the wavelength of x-rays, and moving electrons, protons and neutrons,

- d is the spacing between the planes in the atomic lattice, and

- θ is the angle between the incident ray and the scattering planes.

Waves that satisfy this condition interfere constructively and result in a reflected wave of significant intensity, causing a peak in the pattern diffraction.

The pattern of powder diffraction peaks can be used to quickly identify materials (thanks to the zeolite pattern database [13]), and changes in peak width or position can be used to determine crystal size, crystallinity of zeolites.[12]

The crystallinity of zeolite can be derived from XRD as follow:

$$\text{Crystallinity } (\%) = \frac{\text{Intensity of peak}_{(hkl)} \text{ sample}}{\text{Intensity of peak}_{(hkl)} \text{ reference}} \times 100 \tag{2.2}$$

The crystal size, a is calculated according to Scherrer's equation:

$$a = \frac{0.91\lambda}{\beta \cos\theta} \tag{2.3}$$

Where, β is the full width at half maximum of the corresponding peaks. However, as noticed by Jacobsen et al,[14] the large crystals contribute more to the average size determined by XRD than the small crystals. Hence, crystal sizes determined from XRD of very small zeolite crystals are not very accurate and should be taken as first approximations to the true crystal size.

In a typical test, zeolite sample was characterized by powder wide-angle XRD, recorded on a Siemens D5000 X-ray diffractometer using CuK_α radiation (λ = 1.54184 Å). The samples were scanned over a range of 2θ values from 5 to 50^o with a scan step size of 0.02^o and a scan step time of 1 s.

2.2.6. ^{29}Si Magic Angle Spinning Nuclear Magnetic Resonance Spectroscopy (MAS NMR)

The ^{29}Si MAS NMR spectroscopy now belongs among the most powerful techniques for the characterization of molecular sieves such as zeolites and related materials. The basis of this success was the invention of effective line narrowing techniques and two-dimensional experiments that make the detection of highly resolved solid-state NMR spectra and the separation of different spectral parameters possible. The technique

allows the direct investigation of the framework of zeolites and related materials, of extra-framework cations and of the different types of hydroxyl groups.[15]

Lippmaa et al were among the first to show that the chemical shifts of the ^{29}Si in solid silicates were approximately equal to the chemical shifts of species in solution. Therefore it is easy to differentiate between $Si(OSi)_4$ (Q^4), $(HO)Si(OSi)_3$ (Q^3), $(HO)_2Si(OSi)_2$ (Q^2) silicate species because the chemical shifts lie approximately 10 ppm apart (Q^4 at -110 ppm, Q^3 at -100 ppm, Q^2 at -90 ppm etc).[16] The ^{29}Si MAS NMR technique is also useful when investigating the incorporation of organosilane species. Exchange of one Si-O bond against a Si-C bond (the transformation of a Q-silicon into a T-silicon) causes a shift of about 45 ppm and again there is a separation of approximately 10 ppm between the silicon T^3 $RCSi(OSi)_3$, T^2 $(RC)_2(SiOSi)_2$ and T^1 $(RC)_3SiOSi$. Thus T^3 can be found close to -110 + 45 = -65 ppm T^2 = -100 + 45 = -55 ppm and T^1 at -90 + 45 = 45 ppm.[17]

For measurement, ^{29}Si MAS NMR spectra were recorded at a frequency of 59.60 MHz using 30 o pulses of 3 μs duration, 2600 scans and 30 s recycle delays at room temperature on a Bruker ASX 300 spectrometer.

2.2.7. Scanning electron microscope (SEM)

Scanning electron microscope (SEM) is a microscope that uses electrons rather than light to form an image. As the primary electron beam “scans” across the sample, the electrons on the surface of the sample are excited. This excitation leads to the emission of the secondary electron beam from the surface which produces the image. The SEM can produces images of high resolution, which means that closely spaced features can be examined at a high magnification. Images obtained from this technique can provide information about the surface and particle size of the samples. Preparation of the samples is relatively easy since most SEMs only require the sample to be conductive. In this study, a JEOL JSM-840 scanning electron microscope operated at 15 kV was used.

2.2.8. Transmission Electron Microscope (TEM)

Unlike the SEM technique, where electrons are detected by beam emission, transmission electron microscopy (TEM) make use of the electron beam that has been partially transmitted through the very thin (and so semitransparent for electrons) specimen. This beam is detected to provide the image of the sample. TEM allows investigating the information about the inner structure of the specimen as well as their particle size. Generally, the TEM resolution is about an order of magnitude better than the SEM resolution. All the TEM images reported in this thesis were obtained on a JEOL 2011 transmission electron microscope.

2.2.9. Nitrogen Adsorption/Desorption Isotherms

The isotherms of nitrogen adsorption and desorption at 77K is the technique which has been often used for surface characterization of zeolites. It can provide information about: specific surface, external surface, internal surface as well as the diameter of the mesopores (if available). According to IUPAC, the isotherms are classified into six groups as shown in Figure 2.7. The isotherms of zeolites fall into the type I group. This group are distinguished by a plateau which is nearly or quite horizontal, and which may cut the P/P_o = 1 axis sharply or may show a "tail" as saturated pressure is approached.[18]

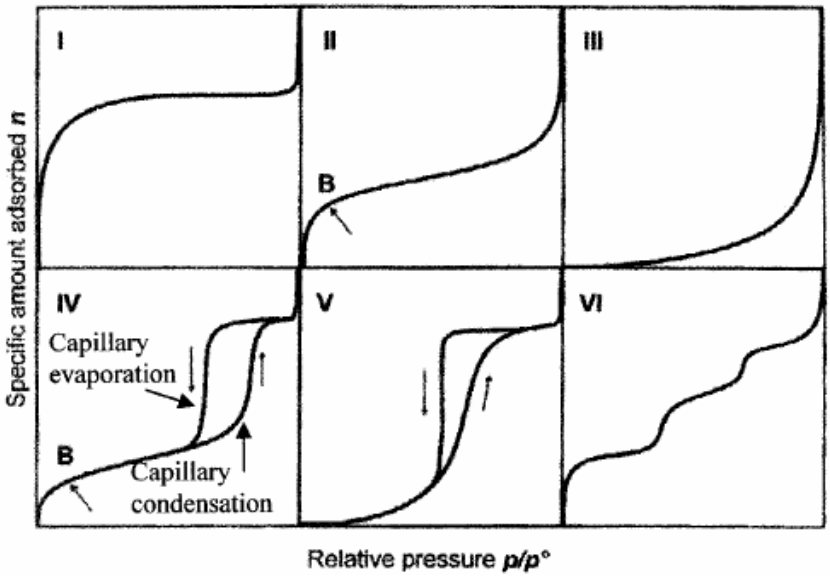

Figure 2.7. Types of sorption isotherms.[18]

The specific surface area of the specimen is derived from the isotherm using BET equation:[19]

$$\frac{p/p_0}{V\left(1-p/p_0\right)} = \frac{1}{V_m C} + \frac{C-1}{V_m C} * \frac{p}{p_0} \tag{2.4}$$

Where,

- V is the volume adsorbed,

- V_m is the volume adsorbed on a monolayer

- P is the pressure of the gas

- P_o is the saturation pressure of adsorbates at the temperature of adsorption

- c is the BET constant, which is expressed by: $c = \exp\left(\frac{E_1 - E_L}{RT}\right)$. E_1 is the heat of adsorption for the first layer, and E_L is that for the second and higher layers and is equal to the heat of liquefaction.

Equation (2.4) can be plotted as a straight line with $1/v[(P_o/P) - 1]$ on the y-axis and P/Po on the x-axis according to experimental results. This plot is called a BET plot. The linear relationship of this equation is maintained only in the range of $0.05 < P/Po < 0.30$. The value of the slope and the y-intercept of the line are used to calculate the monolayer adsorbed gas quantity V_m (reduced in STP) and the BET constant c. Thus the specific surface area S is given by:

$$S = \frac{V_m}{22414} a_m L \times 10^{-20} \text{ [m}^2\text{/g]} \tag{2.5}$$

where, a_m is the average area occupied by a molecule of adsorbate in the completed monolayer for nitrogen $a_m = 16.2$ Å^2 and L is the Avogadro constant.

The external surface area which is strongly dependent on the particle size of zeolites is calculated from the isotherm using t-plot method. This method was developed by de Boer et al.[20, 21] It assumes that during the adsorption when the micropores are already filled-up, the adsorption proceeds to occur on the external area. This stage of adsorption can be regarded as an adsorption on a flat surface. Then the adsorption within this pressure region may be described by a simple linear dependence:

$$a\left(\frac{P}{P_o}\right) = a_{micro,\max} + k.S_{ext}t\left(\frac{P}{P_o}\right) \tag{2.6}$$

where:

- $a\left(\frac{P}{P_o}\right)$: volume adsorbed, reduced to STP,

- $a_{micro,max}$ - adsorption in saturated micropores, corresponding to total volume of micropores,

- S_{ext} - "external" surface area; here it is the surface area of pores larger than micropores,

- $t\left(\frac{P}{P_o}\right)$ - estimated statistical thickness of adsorbed layer, according to Harkins et al.[22] : $t\left(\frac{P}{P_o}\right) = \left(\frac{13.99}{0.034 - \log\frac{P}{P_o}}\right)^{1/2}$

- k - coefficient which depends on units used for the values of adsorption a, layer thickness t and surface area S_{ext}, e.g. for t [nm], S [m^2/g] and a [cm^3/g STP] we obtain: k = 0.6489.

The t-plot is illustrated in Figure 2.8.

In this study, the nitrogen adsorption/desorption measurements were carried out using an Omnisorp-100 automatic analyser at -196 ^{o}C after degassing about 30 mg of calcined sample at 200 ^{o}C for at least 4 h under vacuum (10^{-4} -10^{-5} torr).

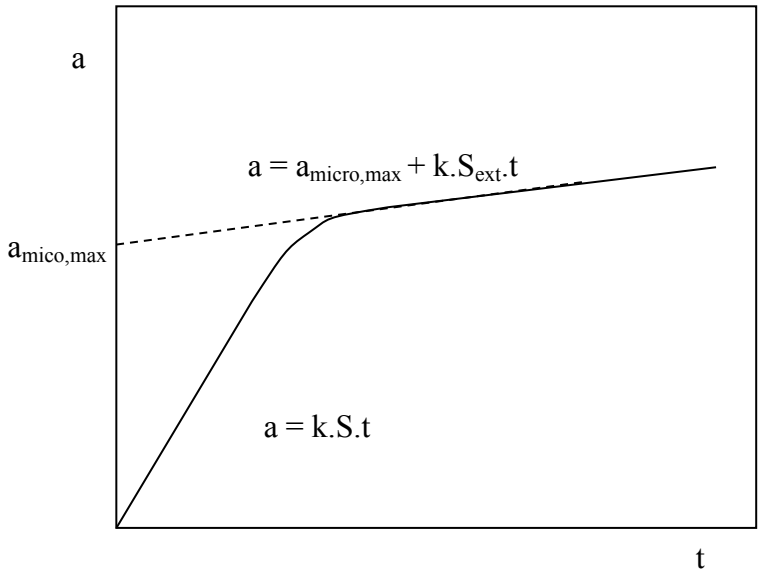

Figure 2.8. t-plot method.

2.2.10. Cracking reaction

Cracking experiments were performed in an automated fixed-bed microactivity test (MAT) unit (Zeton Automat IV), which was a modified version of ASTM D 5154. The unit was equipped with collection systems for gas and liquid products. The distribution of gaseous products was analyzed by gas chromatographies. The boiling point (bp) range of the liquid products was determined by simulated distillation gas chromatography.

The catalysts were tested in the MAT unit at 510 °C with a weight hourly space velocity (WHSV) of 8 h^{-1}. MAT results reported include conversion, yields of dry gas (H_2, H_2S, C_1 and C_2), liquefied petroleum gas (LPG, i.e., C_3-C_4), gasoline (> C_5, bp up to 215 °C), LCO (bp 215-345 °C), heavy cycle oil (HCO, bp above 345 °C) and coke. Conversion was determined from the difference between the amount of feed and the amount of

unconverted material defined as liquid product boiling above 215 °C (i.e., LCO + HCO). The same vacuum gaz oil (VGO) was used to all MAT runs